Controlled Power Sequencing for Fault Protection in DC Nanogrids

P. Cairoli, I. Kondratiev, and R. A. Dougal
University of South Carolina, Columbia, SC, USA
pietro.cairoli@gmail.com

***Abstract*—For dc power distribution systems, we show how coordinated operation of electronic power converters and mechanical contactors (segmentizing switches) can permit rapid response to short circuit faults. It is possible to de-power the dc bus, open a contactor to isolate the faulted branch, then restore power to the remaining branches in less than 8 ms, so that the remaining loads can ride through the entire operation. This is faster than can typically be achieved in ac power networks using conventional technologies. Clamping diodes and point of load capacitors improve system robustness. Our results provide a detailed analysis, design guidelines, and explain how the protection scheme responds to different configuration of the system.**

***Index Terms*—DC Nanogrid, fault protection, Power electronics, converters control.**

I. Introduction

The increasing performance, higher efficiency, and decreasing cost of power electronic converters have spurred a rediscovery and proliferation of dc distribution systems [1, 2], and these are especially of interest in renewable energy systems which often have no inherent 50/60 Hz ac nature. Instead simple dc/dc converters are sufficient to interface sources and loads to the system [3].

Although dc offers advantages such as improved transmission efficiency and ease of interfacing asynchronous sources, the protection of dc distribution systems against short circuit line fault and ground fault is still under discussion, especially for distribution systems and multisource nanogrids.

Traditionally arcing-type circuit breakers are the most common form of protection method for any power nanogrid such as that shown in Figure 1 on a representative example of multisource nanogrid that contains several sources, storage elements, distribution buses, and loads. The figure also shows locations of circuit protection elements needed to protect the nanogrid against short circuit faults along with some representative locations of faults that could occur in the system.

Ac breakers provide feasible solution for nanogrid protection because alternating currents naturally cross zero at every half-period, thereby creating conditions for self-extinguishing of arcs within mechanical circuit breakers. In a dc system, there are no such natural zero crossings and therefore currents must be forced to zero by external means before mechanical switches can be opened [4]. In addition, the magnitude of a fault current might be quite large, being limited only by the resistance of the system, rather than by inductive impedance as in ac systems. For these reasons, mechanical circuit breakers that should open against such fault currents require special design methods that become impractical at higher voltages and currents [5, 6].

The contribution of this paper is a fault protection method that is suitable for multisource nanogrids, limits the intensity of fault currents, reduces the time to eliminate the fault, and allows loads to ride through the process uninterrupted.

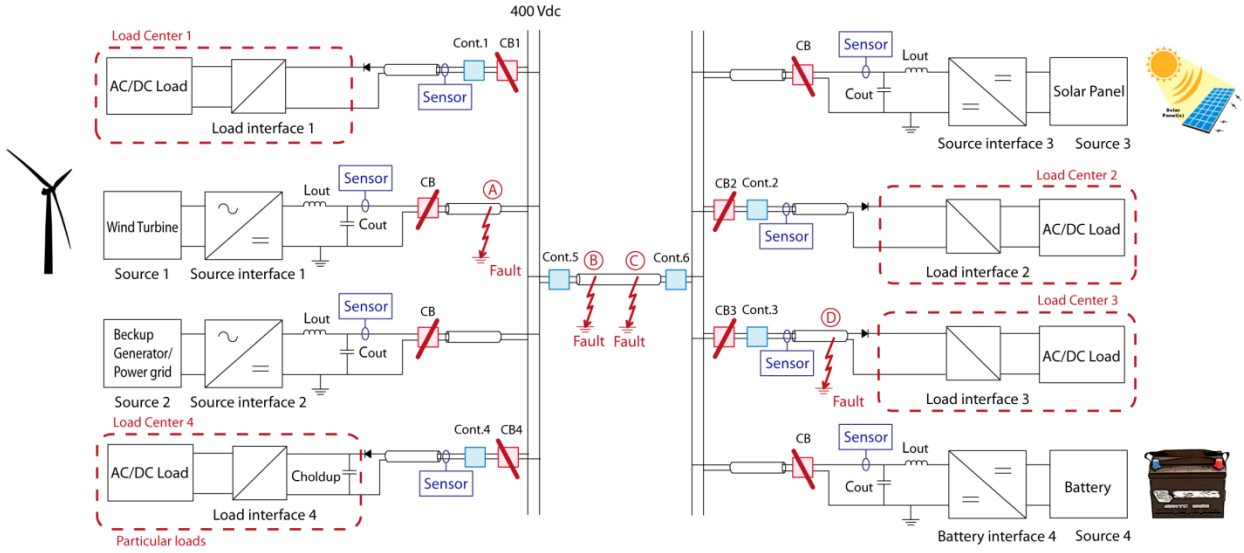

Fig. 1. Structure of a typical renewable dc nanogrid.

Our approach eliminates dc circuit breakers, in favor of simpler, smaller grid segmentizing contactors, by coordinating the action of these contactors with the action of electronic power converters that are commanded to briefly de-energize the distribution grid, so that the contactors are able to isolate the faulted branch and reconfigure the remaining network [7]. Following industry standards for power quality, power disruptions shorter than 10 ms are permissible, and these are used to permit contactor operation and reconfiguration [8, 9].

We will first illustrate the proposed protection approach, then explore the fault dynamics and the dependence of fault current behavior on physical dimensions of the grid, number of sources, and fault location. Then we will analyze the influence of system parameters on the performance of the protection scheme and present design considerations, and limitation of components and system parameters as well as considerations on selection of contactors for reconfiguring the nanogrid, on ride-through capability for loads, and power quality.

II. Operation of the Protection

According to our approach, power converter settings and contactor activation signals should be operated according to the following sequence after a fault is identified:

1) The current limit set points of converters that feed the nanogrid are reset to zero)

2) As soon as the fault current decays to the rated contactor opening current, but before the current is actually zero, appropriate contactors are actuated to reconfigure the system and to isolate the faulted branch. This operating mode takes advantage of the forward voltage of the low-current inter-contact arc to more-rapidly drive system current to zero.

3) After current is driven to zero and any other contactors are repositioned to effect any desired system reconfiguration, the nanogrid is re-energized.

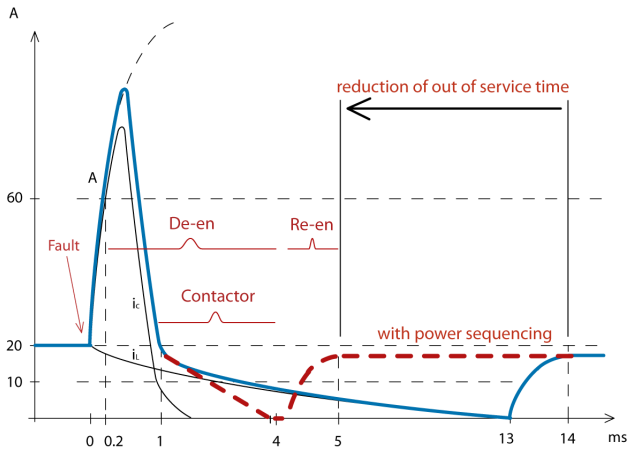

Fig. 2. Controlled power sequencing fault elimination.

Figure 2 shows notional current waveforms associated with this controlled power sequencing approach corresponding to the case when a short circuit occurs in the cable serving load 3 of Fig 1. The red dotted waveform shows how rapidly the system can be reconfigured and power can be restored to a healthy branch of the system, whereas the solid line shows the longer time that would be needed to recover system operation if the controlled sequencing were not used to take advantage of the forward arc voltage of the contactor to help in driving the current to zero. Without this arc voltage, the current decay rate is determined only by the equivalent RL time constant of the fault path (eg. 13 ms) [10].

The bus current, measured at the ends of the common bus, exhibits two main transient behaviors, as illustrated by the black lines in Figure 2: a fast peak i_C due to the discharge of filter capacitors and a slow decaying behavior i_L due to the discharge of filter inductors. During the first interval (t = 0 - 1 ms), the current increases rapidly as energy stored in the output capacitors of the converters are discharged. After this rapid discharge, during the second time interval (t = 1 – 13 ms), the current decays more slowly, as the filter inductor of the main converter is discharged. Two important features of the proposed protection scheme are (1) the reduction of the fault current by limiting the energy discharged into the fault to the only energy of filter components by control of converters, and (2) the shortening of the out of service time via coordination and control of converters and contactors.

If a fault occurs in load branch 3 of Figure 1, the protection system operates as follows: first the fault is identified and the feeding converters connected to the bus are turned off; next, the energy accumulated in the output capacitor of converters is dissipated, and the fault current becomes the contribution of the inductive components of the path between sources and the fault; finally, once the fault current drops below the rated opening current of the contactor 3, the contactor 3 opens and the fault is isolated. At this point, the sources can be turned back on.

As we can see from Figure 2, the out of service time can be significantly reduced.

III. Fault Dynamics

In general, multi-source nanogrids represent a complex dynamic system, transients of which depend on the systems parameters. In this section, using simplifying assumptions, we, first, find estimates of important parameters for the protection operation, such as peak fault current and time for safe contactor opening. Then, using a detailed model of the system, we verify the obtained estimates by simulation of a nanogrid system with four power sources under variable cable length.

A. System model during the fault

As shown in Figure 2, during the fault, under the proposed protection the system goes through a number of operation phases:

- fault identification (from the moment of fault until fault is identified)
- bus de-energizing (fault identified and power converter operation is blocked);
- faulty branch isolation (a contactor physically isolate the part of the system affected by a short circuit fault)
- bus re-energizing (converters are turned back on and supply power to loads)

These operation phases directly correspond to different system topologies. For simplicity of the analysis, we assume that time for identifying the fault is negligible and the system goes directly into the second phase; and a linear model of the system provides us with sufficient accuracy of the estimates.

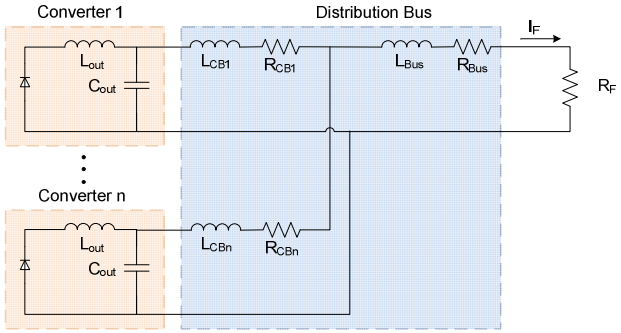

Fig. 3. Nanogrid equivalent circuit during a fault.

During the second phase, the simplified nanogrid schematic is shown in Figure 3, where we used cable representation that takes into account only inductive and resistive behavior. The dynamic model of the simplified system can be written as follows:

$$\begin{cases} \frac{di_{Lj}}{dt} = \frac{1}{L_{outj}}\left(V_{gj} - V_{Coutj}\right) \\ \frac{dv_{Cj}}{dt} = \frac{1}{C_{outj}}\left(i_{Lj} - i_F\right) \\ \frac{di_{Fj}}{dt} = \frac{1}{L_{CBj}}\left(V_{Coutj} - R_F i_F\right) \end{cases} \quad (1)$$

$$i_F = \sum_{j=1}^{n} i_{Fj} \quad (2)$$

As it can be seen from equation (2), the fault current is a composition of currents supplied through all of the individual converters. Moreover, as it can be seen from figure 2 that fault current (i_F) consists of two components with fast (i_{Ff}) and slow (i_{Fs})dynamics as shown in (3)

$$i_F = i_{Ff} + i_{Fs} \quad (3)$$

In our analysis we use this separation of the system dynamics to simplify the obtained results.

B. Peak fault current

Since during the second phase of operation the system bus is disconnected from the primary sources, the energy dissipated in the fault is limited to the energy accumulated in the system's reactive components such as converters' output capacitors C_{OUT} and inductors L_{OUT}, and cable inductance L_{CB}. It is clear that peak fault current depends on the configuration of the system, the location of the fault, and the operating conditions when fault happens.

We start from the analysis of a peak fault current in a single source system. For a one source system, the system model can be written as follows:

$$\begin{cases} \frac{di_L}{dt} = \frac{1}{L_{out}}\left(V_g - V_{Cout}\right) \\ \frac{dv_C}{dt} = \frac{1}{C_{out}}\left(i_L - i_F\right) \\ \frac{di_F}{dt} = \frac{1}{L_{CB}}\left(V_{Cout} - R_F i_F\right) \end{cases} \quad (4)$$

To simplify the analysis assume that converter inductor is significantly larger than the cable inductance and the fault current consists of fast and slow dynamics as shown in (3). This assumption reduces the system (4) to system shown in (5) and allows us to consider fast and slow transients separately. The fast transients correspond to discharge of the output capacitor through the fault and slow transients are driven by the output filter inductance of the converter.

$$\begin{cases} \frac{di_{Ff}}{dt} = \frac{1}{L_{CB}}\left(v_C - i_{Ff} R_F\right) \\ \frac{dv_C}{dt} = -\frac{1}{C_{out}}\left(i_{Ff}\right) \\ \frac{di_{Fs}}{dt} = -\frac{1}{(L_{out}+L_{CB})} i_{Fs} R_F \end{cases} \quad (4)$$

Arranging system (4) as one second order equation with respect to i_{Ff}we get the following equation:

$$\begin{aligned} &L_{CB} C_{out} i''_{Ff} + C_{out} R_F i'_{Ff} + i_{Ff} = 0 \\ &(L_{out} + L_{CB}) i'_{Fs} + R_F i_{Fs} = 0 \end{aligned} \quad (5)$$

The evolution of the fault current is defined by expression (6).

$$\begin{aligned} &i_{Ff}(t) = C_1 e^{p_1 t} + C_2 e^{p_2 t} \\ &i_{Fs}(t) = C_3 e^{p_3 t} \end{aligned} \quad (6)$$

With:

$$p_{1,2} = \frac{-C_{out} R_F \pm \sqrt{\left(C_{out}^2 R_F^2 - 4 L_{CB} C_{out}\right)}}{2 L_{CB} C_{out}}$$

$$p_3 = -\frac{R_F}{(L_{out}+L_{CB})}$$

$$C_1 = i_{Ff}(0) - C_2$$

$$C_2 = \frac{(v_{Cout}(0) - i_{Ff}(0)R_F - i_{Ff}(0)L_{CB}p_1)}{L_{CB}(p_2 - p_1)}$$

$$C_3 = i_{Fs}(0)$$

Using equations (6), time of the maximum fault current and maximum fault current can be found as shown in equation (7).

$$t_m = \frac{ln\left(-\frac{C_1 p_1}{C_2 p_2}\right)}{p_2 - p_1}$$
$$i_{Fmax} = i_{Fs}(t_m) + i_{Ff}(t_m) \quad (7)$$

Expressions (6) and (7) clearly show complexity of the dependency of peak fault current on the system reactive components. From (6) it follows that the rate of increase of fault current is inversely proportional to the value of the cable inductance.

Applying a similar procedure to the multi-source system, and assuming that all the primary sources have similar power ratings, we obtain approximation (8) of the fault current behavior for the case on *n* parallel power sources.

$$i_{Fmax} = \sum_{j=1}^{n} i_{Fmaxj}(t_m) \quad (8)$$

C. Proper contactor opening time and dynamics

Very important parts of the coordination between power converters and contactors are the time the contactor start opening and the arc voltage across the contacts of the contactor.

Opening the contactor at precisely the right time is one of the key elements of this scheme. The proper time can be found by solving equation (6) for the time at which the slow part of the current decreases to the rated operating current of the contactor. We find this time by solving the following equation:

$$i_{Fs}(t_{cn}) = C_3 e^{p_3 t} = I_{cn} \quad (9)$$

where I_{cn} is nominal current that contactor can open. The solution of (9) is presented in (10).

$$t_{cn} = \frac{(L_{out} + L_{CB})}{R_F} \cdot ln(i_{Fs}(0)/I_{cn}) \quad (10)$$

where $i_{Fs}(0)$ stands for initial fault current that equals or less than rated current of the system (i_r).

The arc voltage across the two contacts of a contactor causes the fault current to decrease faster than the natural decay rate for the equivalent RL circuit of the fault current path. Considering the system in the slow dynamic, the following equivalent circuit (Figure 4) can be used to study the fault current decaying forced by the contactor [11].

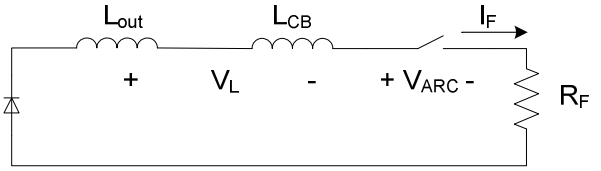

Fig. 4. Equivalent circuit during contactor opening.

During the opening of the contactor the following dynamic takes place:

$$v_L = (L_{out} + L_{CB})\frac{di_F}{dt} = -R_F i_F - V_{ARC} \quad (11)$$

And the solution of the differential equation (11) can be found in equation (12).

$$i_F(t) = C_4 e^{p_4 t} - \frac{V_{ARC}}{R_F} \quad (12)$$

where:

$$C_4 = I_{cn} + \frac{V_{ARC}}{R_F}$$

$$p_4 = -\frac{R_F}{(L_{out} + L_{CB})}$$

The duration of time of the arcing process (t_{ARC}) is defined by expression (13), and the time to totally extinguish the fault current (t_{ex}) is shown by equation (14).

$$t_{ARC} = \frac{1}{p_4} ln\left(\frac{V_{ARC}}{C_4 R_F}\right) \quad (13)$$

$$t_{ex} = t_{cn} + t_{ARC} \quad (14)$$

D. System Performance from Simulation

Using a 400Vdc, 10kW nanogrid dc distribution system similar to the one presented in Figure 1, we compared estimates for peak current (i_{Fmax}) and safe time for contactor opening (t_s) obtained through the analysis with simulation results obtained using Matlab/Simulink. The nanogrid is composed of four different types of sources each having a rated power of 10kW. Each source is connected to the nanogrid through an electronic power converter. While a number of means for fault detection exists, in our simulation we have used a simple threshold based fault detection.

In the model, we considered a RL representation of the cable, different values of output filter inductance and capacitance of the feeding converters, different number of converters connected to the distribution bus. Load centers have been represented by equivalent resistive loads. Table I shows the value of cable parameters for different lengths of the dc distribution bus. Selection of cables has been carried out by considering a constant voltage drop across the distribution grid ($\Delta V = 5\%$ for each of the two conductors). This leads to a slight variation of the resistance component and a consistent increasing of the

inductance component with increasing length of the bus cable.

TABLE I
CABLE PARAMETERS

length [m]	section [mm^2]	ΔV [V]	r [Ohm/m]	l [mH/m]	R_{CB} [Ohm]	L_{CB} [mH]
50	1.5	5%	0.0148	0.000176	0.592	0.022409
70	2.5	5%	0.00891	0.000168	0.6237	0.037433
100	4	5%	0.00557	0.000155	0.6684	0.059206
200	6	5%	0.00371	0.000143	0.6678	0.081933
300	10	5%	0.00224	0.000135	0.672	0.128916
500	16	5%	0.00141	0.000112	0.705	0.178254
1000	25	5%	0.000889	0.000106	0.889	0.337408
1500	35	5%	0.000641	0.000111	0.9615	0.529986
2000	50	5%	0.000473	0.000101	0.946	0.642986

The length of the distribution bus strongly influences the fault current behavior. In particular, there is a parallel relationship between the length of the bus and the inductive component. This causes the current peak to decrease its maximum value and to increase its duration. Figure 5 shows the current peak right after a fault for different length of the grid. Although a wide grid limits the fault current peak magnitude, the time for the current to go down under the nominal current value of a specific branch increases, and thus the time for a safe tripping of the contactor increases. However, also for wide grid (up to 2 km), the time for a safe tripping of contactors remains within 0.6 - 1 ms. This time is consistent with the opening speed of mechanical contactors, which typically require ~ 1ms for the contacts to separate sufficiently to generate appreciable arc voltage.

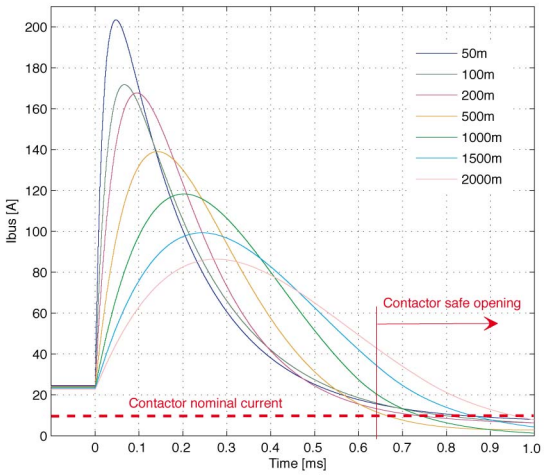

Fig. 5. Fault current dependence on the length of the transmission line.

Considering a multisource nanogrid of roughly 200-meter size, we tested the performance of the system for faults occurring in several different locations that were identified in Figure 1 as (A, B, C, D). Despite the fact that the current peak increases with proximity to the source, we can observe that after a certain time (e.g. within 1 ms), for each fault location, the fault current falls to a value less than the nominal current of each branch connected to a load center. Figure 6 shows the behavior of the fault current for different distances of the fault from the sources 1, 2 on the left of the schematic. The contactor nominal current line corresponds to the rated dc closing or opening current of the contactor.

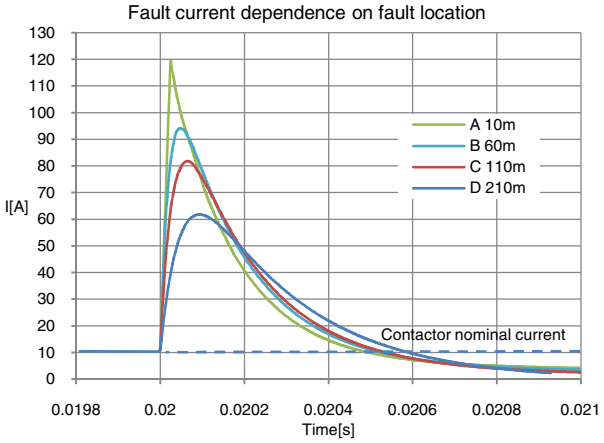

Fig. 6. Fault current dependence on fault location.

Under the hypothesis that each load center is interfaced with the rest of the grid by means of a contactor, when the fault current falls under the nominal value of the associated part of the system, contactors can physically isolate the faulted part of the nanogrid.

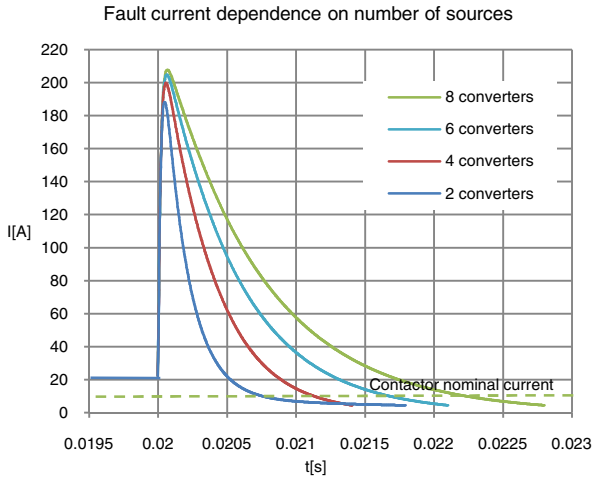

Fig. 7. Fault current dependence on number of sources.

Moreover, the current peak due to a short circuit fault is strongly influenced by the size of filter capacitance and inductance connected to the bus, and thus on the number of sources feeding the bus at the moment of the fault. Figure 7 illustrates the fault current dynamic for an increasing number of paralleled power sources, each of those connected through an electronic power converter. There is a parallel relationship between the number of

connected sources and the time to cross the appropriate value of the current at which the contactor should be opened.

IV. Protection Scheme Performances

Utilizing the same nanogrid model, we studied the performance of the protection system when a short circuit fault happens, in order to validate the application of the approach in a dc nanogrid environment.

A. Transient behavior

In simulations, in order to consider the dynamics of the contactors, we represented it as an ideal switch with in parallel a constant voltage source (V_{ARC}) and a diode as shown in Figure 8. As a first approximation we considered a 100 V arc voltage.

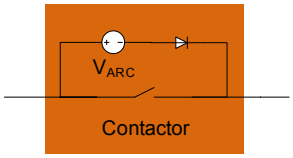

Fig. 8. Contactor modeling for simulations.

In this way, we neglect the mechanical dynamics by introducing an operation delay of the ideal switch, with the assumption that in 3 ms a fast mechanical contactor is able to move its contacts as shown in experimental study presented in [12].

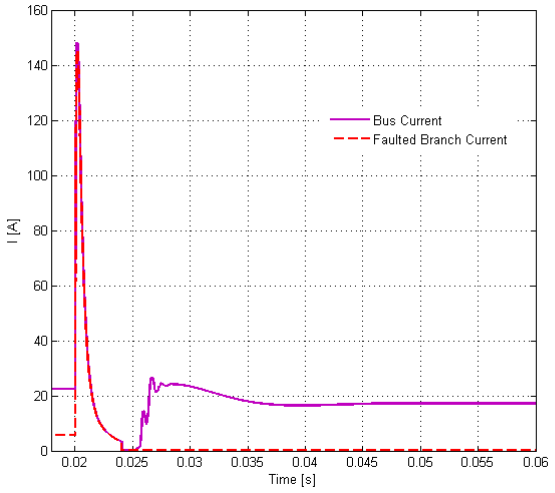

Fig. 9. Bus current behavior during a short circuit fault

When a fault happens (t = 0.02 s) and the current goes over a tripping threshold, converters that feed the bus are turned off, the current accumulated in inductors and capacitors discharges into the fault. When the fault current goes down under the nominal current value of the faulted branch a contactor opens and the fault is physically isolated (t = 0.024 s). Once the fault current is extinguished and the fault isolated, converters turn back on, the bus is re-energized and loads go back to normal operation. Figure 9 shows the bus current behavior in a typical intervention due to a short circuit fault in one of the branches of the grid. The solid line represent the current in the part of the bus that can be reconfigured, and the dashed line shows the current in the faulted part of the grid.

Figure 10 illustrates the voltage outage during a fault; the blue solid line represents the voltage on a healthy load (Vload1), and the green dotted line shows the behavior of the voltage on a load with a hold-up capacitor installed and isolated by a diode (Vload4). In this example we considered load 4 as a 2.5 kW load sustained by a 100 µF capacitor for 10 ms.

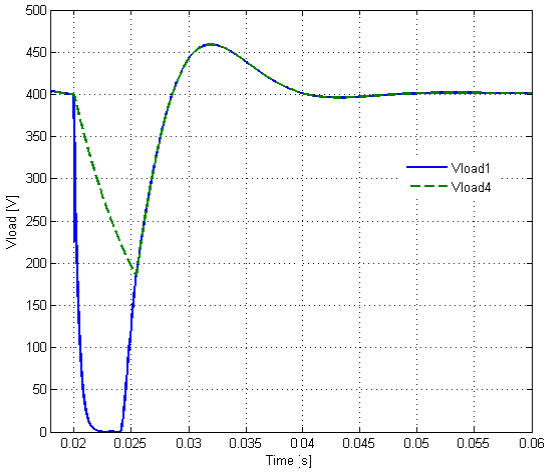

Fig. 10. Voltage outage during a short circuit fault

The following expression gives an approximation of the size of hold-up capacitors:

$$C_{hold-up} = \frac{2 \cdot P_{load} \cdot t_{out}}{V_n^2 \cdot 0.7} \qquad (15)$$

Where V_n is the nominal voltage of the dc bus and P_{load} is the power request of the load of the relative load center. The 0.7 coefficient indicates that the minimum allowed voltage of the capacitor is 70%.

B. Operating time

Time to complete isolation of the fault depends also on the contactor operating time.

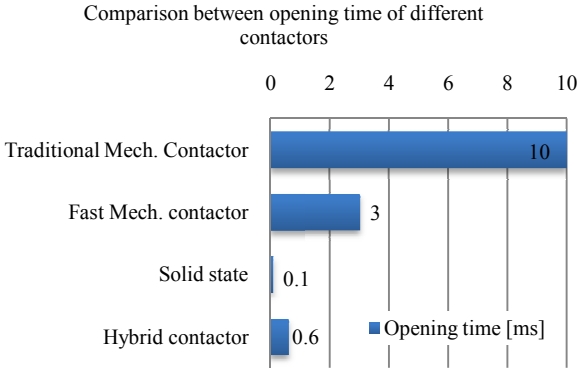

Fig. 11. Opening time for different kind of contactors.

Contactor operation times range from a few milliseconds for solid state or hybrid contactors to about ten milliseconds for of shelf mechanical contactors [13-15]. Figure 11 shows a comparison between different type of contactors and their opening times.

Figure 12 illustrates the performance of the protection scheme depending on the number of sources connected to the grid and, thus, for different amounts of total capacitance connected to the dc nanogrid, and by using fast mechanical contactors to isolate the faulted part of the nanogrid. The first interval corresponds to the time to de-energize the bus, the second interval is the time to isolate the fault, and the last represent the time to reconfigure the nanogrid, and bring the system to normal operation.

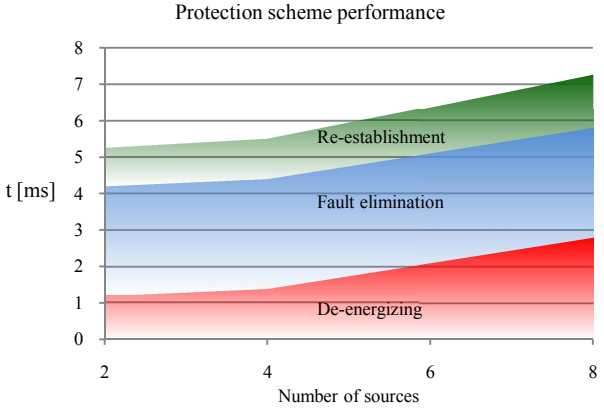

Fig. 12. Performance of the protection scheme.

The selection of fast mechanical contactors allows the system to be protected and reconfigured within 8 ms, in such a way that fault in invisible to loads, also for the critical condition of 8 sources connected to the grid. In case of slower mechanical contactors, to provide ride through capability for loads we have to consider hold-up capacitors to supply power during the time that the lone is down.

C. *Power quality*

According to Figure 13 that shows the design characteristics of common ac loads and load voltage tolerance for MVDC distribution systems, the obtained reduction of out of service time introduces robustness against short power interruptions. In fact a voltage outage shorter than 10 ms does not affect load operation and falls within allowable power quality requirements. The black line shows the limit for a voltage variation to affect the load performance in a traditional ac system, and the green zone identifies the boundaries of voltage sag and overvoltage for the operation of dc loads [8, 9]. The blue line represents the range of voltage outage durations when the system is protected with our method. We can observe the variation range of the duration of voltage outages (blue area). The shorter duration is determined by short lines and few sources connected to the dc bus; the longer duration is caused by wide grid dimension and high number of connected sources at the moment of the short circuit fault.

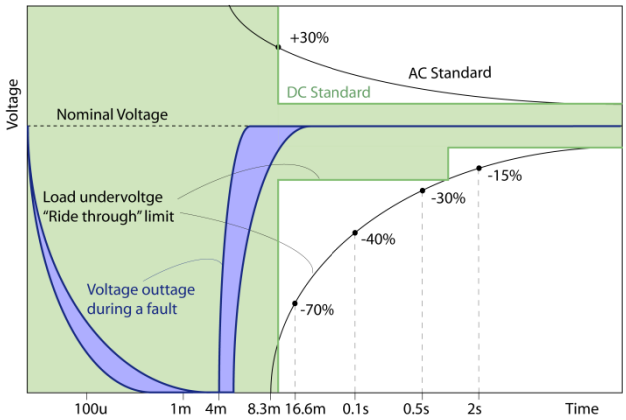

Fig. 13. Load sensitivity to voltage sags.

In cases when the out of service time is greater than 8-10 ms some loads will experience excessive voltage sags which may require the addition of load hold-up capacitors in these load zones. The introduction of capacitors that are close to the loads and protected by a diode permits loads to ride-through the process uninterrupted also for outages of longer duration. An example of hold-up capacitor location is shown at load center 4 in Figure 1. Guidelines to design the size of hold-up capacitors have been presented in (15) and also in previous works [7].

V. Conclusions

We have shown that a power sequence control scheme can be used to protect and reconfigure a nanogrid dc distribution system in response to short circuit line faults. Results of our study show that it is possible to eliminate the fault and re-energize the line faster than an ac grid can be protected and reconfigured using traditional circuit breakers, and ride-through capability for loads can be provided.

We show how the de-energizing and reconfiguration times depend on the number of sources connected to the grid, on the distance to the fault, and the performance of contactors that isolate faulted parts of the system. Our results provide essential guidelines for design of fault protection for nanogrid dc power systems using power sequencing and they illustrate how to achieve specified reaction times of the protection scheme.

Acknowledgment

The authors are grateful for support of the US Office of Naval Research under grant N00014-08-1-0080.

References

[1] Mesut E. Baran, Nikhil R. Mahajan, "DC Distribution for industrial systems: opportunities and challenges", IEEE Transactions on industry application, vol. 39, NO. 6, November/December 2003

[2] S. R. Rudraraju, A. K. Srivastava, S. C. Srivastava, N. N. Schulz, “Small signal stability analysis of a shipboard MVDC power system”, IEEE 2009
[3] J. Schoenberger, R. Duke S. D. Round, “DC-Bus Signaling: a distributed control strategy for a hybrid renewable nanogrid”, IEEE Transactions on industrial electronics, Vol. 53, No. 5, October 2006
[4] Fang Luo, Jian Chen, Xinchun Lin, Yong Kang, Shanxu Duan, “A novel solid state fault current limiter for DC power distribution network”, IEEE 2008
[5] J. G. Ciezki, R. W. Ashton, “Selection and stability issues associated with a navy shipboard DC zonal electric distribution system”, IEEE Transactions on power delivery, Vol. 15, NO. 2, April 2000
[6] A.Ouroua, J.Beno, R.Hebner, “Analysis of fault events in MVDC architecture”, IEEE 2009
[7] P. Cairoli, R. A. Dougal, U. Ghisla, I. Kondratiev, “Power sequencing approach to fault isolation in dc systems: Influence of system parameters”, IEEE ECCE 2010
[8] Jerry C. Whitaker, “AC Power system handbook, Third Edition”, CRC Press, 2007
[9] IEEE Recommended Practice for 1kV to 35kV Medium-Voltage DC Power System on Ship – IEEE Std 1709-2010
[10] P. Cairoli, I. Kondratiev, R. Dougal, “Ground Fault Protection for DC Bus Using Controlled Power Sequencing”, IEEE SoutheastCon 2010
[11] T. Robbins, “Circuit-Breaker Model for Over-Current Protection Simulation of DC Distribution System”, IEEE 1995
[12] J. Tucker, D. Martin, R. Dougal, E. Santi, “Fault Protection and Ride-Through Scheme for MVDC Power Distribution System Utilizing a Supervisory Controller”, IEEE ESTS, April 2011, Alexandria, VA
[13] “A DC Hybrid Circuit Breaker With Ultra-Fast Contact Opening and Integrated Gate-Commutated Thyristors (IGCTs)” – J-M Meyer, A. Rufer – IEEE Transactions on Power Delivery, Vol. 21, No. 2, April 2006
[14] ABB Power Breakers Catalogue 2009
[15] Kilovac Lev200, Tyco Electronics catalogue 2010